Chapter 6
Reduced Basis Isogeometric Mortar Approximations for Eigenvalue Problems in Vibroacoustics

Thomas Horger, Barbara Wohlmuth, and Linus Wunderlich

Abstract We simulate the vibration of a violin bridge in a multi-query context using reduced basis techniques. The mathematical model is based on an eigenvalue problem for the orthotropic linear elasticity equation. In addition to the nine material parameters, a geometrical thickness parameter is considered. This parameter enters as a 10th material parameter into the system by a mapping onto a parameter independent reference domain. The detailed simulation is carried out by isogeometric mortar methods. Weakly coupled patch-wise tensorial structured isogeometric elements are of special interest for complex geometries with piecewise smooth but curvilinear boundaries. To obtain locality in the detailed system, we use the saddle point approach and do not apply static condensation techniques. However within the reduced basis context, it is natural to eliminate the Lagrange multiplier and formulate a reduced eigenvalue problem for a symmetric positive definite matrix. The selection of the snapshots is controlled by a multi-query greedy strategy taking into account an error indicator allowing for multiple eigenvalues.

6.1 Introduction

Eigenvalue problems in the context of vibroacoustics often depend on several parameters. In this work, we consider a geometry and material dependent violin bridge. For a fast and reliable evaluation in the real-time and multi-query context, reduced basis methods have proven to be a powerful tool.

For a comprehensive review on reduced basis methods, see, e. g., [29, 33] or [28, Chap. 19] and the references therein. The methodology has been applied successfully to many different problem classes, among others Stokes problems [20, 22, 32, 34], variational inequalities [13, 15] and linear elasticity [24]. Recently, reduced basis methods for parameterized elliptic eigenvalue problems (μEVPs)

T. Horger (✉) • B. Wohlmuth • L. Wunderlich
Institute for Numerical Mathematics, Technische Universität München, Boltzmannstraße 3, 85748 Garching b. München, Germany
e-mail: horger@ma.tum.de; wohlmuth@ma.tum.de; linus.wunderlich@ma.tum.de

P. Benner et al. (eds.), *Model Reduction of Parametrized Systems*, MS&A 17, DOI 10.1007/978-3-319-58786-8_6

gained attention. Early work on a residual based a posteriori estimator for the first eigenvalue can be found in [23] and has been generalized in [26, 27] to the case of several single eigenvalues with special focus to applications in electronic structure problems in solids. Furthermore, the very simple and special case of a single eigenvalue where only the mass matrix and not the stiffness matrix of a generalized eigenvalue problem is parameter dependent has been discussed in [11]. Alternatively to the classical reduced basis approach, component based reduction strategies are considered in [36]. Here, we follow the ideas of [17] where rigorous bounds in the case of multi-query and multiple eigenvalues are given. More precisely, a single reduced basis is built for all eigenvalues of interest. The construction is based on a greedy strategy using an error estimator which can be decomposed into offline and online components.

The eigenvalues of a violin bridge play a crucial role in transmitting the vibration of the strings to the violin body and hence influence the sound of the instrument, see [10, 37]. Due to the complicated curved domain and improved eigenvalue approximations compared to finite element methods, see [19], we consider an isogeometric discretization. Flexibility for the tensor product spline spaces are gained by a weak domain decomposition of the non-convex domain.

Isogeometric analysis, introduced in 2005 by Hughes et al. in [18], is a family of methods that uses B-splines and non-uniform rational B-splines (NURBS) as basis functions to construct numerical approximations of partial differential equations, see also [1, 5]. Mortar methods are a popular tool for the weak coupling of non-matching meshes, originally introduced for spectral and finite element methods [2, 3]. An early contribution to isogeometric elements in combination with domain decomposition techniques can be found in [16]. A rigorous mathematical analysis of uniform inf-sup stability and reproduction properties for different Lagrange multiplier spaces is given in [4]. Applications of isogeometric mortar methods can be found in [7, 8, 35]. The weak form of a discrete mortar approach can be either stated as a positive definite system on a constrained primal space or alternatively as an indefinite saddle point system in terms of a primal and dual variable. Both formulations are equivalent in the sense that they do yield the same primal solution. From the computational point of view, quite often the saddle point formulation is preferred since it allows the use of locally defined basis functions and yields sparse systems. The elimination of the dual variable involves the inverse of a mass matrix and, unless biorthogonal basis functions are used, significantly reduces the sparsity pattern of the stiffness matrix. In general, the constrained primal basis functions have a global support on the slave side of the interface. This observation motivates us to use for the computation of the detailed solution the saddle point mortar formulation and work with locally defined unconstrained basis functions yielding sparse systems. However, typically a reduced system is automatically dense. If the constraint is parameter independent we obtain a positive definite system for the reduced setting. Here we show that even in the situation of a parameter dependent geometry, we can reformulate the weak continuity constraint in a parameter independent way.

The rest of this contribution is structured as follows. In Sect. 6.2, we introduce the model problem and briefly discuss the assumed orthotropic material law and the applied isogeometric mortar discretization for the violin bridge. The geometric setup includes a thickness parameter which is transformed to a material parameter. Here, we also comment on the fact that although the geometry transformation formally brings in a parameter into the weak mortar coupling, we can recast the problem formulation as a parameter independent coupling condition across the interfaces. The reduced basis approach is given in Sect. 6.3. Finally numerical results illustrating the accuracy and flexibility of the presented approach are given in Sect. 6.4. We point out that our parameter space is possibly non-convex due to the non-linear constraints of the material parameters.

6.2 Problem Setting

The numerical simulation of vibroacoustic applications involves quite often complex domains. Typical examples are large structures, such as, e.g., bridges, technical devices such as, e.g., loudspeakers but also parts of string instruments such as, e.g. violin bridges see Fig. 6.1. Within the abstract framework of modal analysis, the fully bi-directional mechanical-acoustic coupled system can be reduced to a generalized eigenvalue problem.

For the three dimensional geometry of a violin bridge, we consider the eigenvalue problem of elasticity

$$-\operatorname{div}\sigma(u) = \lambda\rho u,$$

where $\rho > 0$ is the mass density, and $\sigma(u)$ depends on the material law of the structure under consideration. In our case, linear orthotropic materials are appropriate since as depicted in Fig. 6.2 wood consists of three different axes and only small deformations are considered. Note that besides the cylindrical structure of a tree trunk, we consider Cartesian coordinates due to the small size of the violin bridge compared to the diameter of a tree trunk.

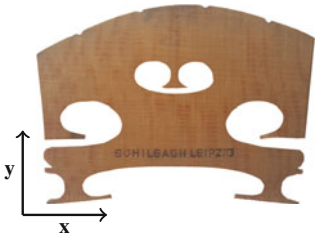

Fig. 6.1 Example of a violin bridge

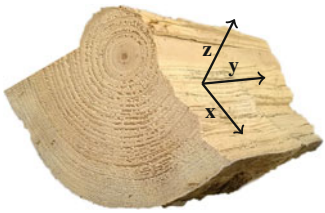

Fig. 6.2 Illustration of the orthotropic structure of wood

6.2.1 Orthotropic Material Law

The three axes are given by the fiber direction y, the in plane orthogonal direction z and the radial direction x. By Hooke's law, the stress strain relation can be stated in its usual form as $\sigma(u) = \mathbb{C}\varepsilon(u)$ with $\varepsilon(u) = (\nabla u + \nabla u^\top)/2$. Due to the alignment of the coordinate system with the orthotropic structure, the stiffness tensor is given as

$$\mathbb{C} = \begin{pmatrix} A_{11} & A_{12} & A_{13} & 0 & 0 & 0 \\ A_{21} & A_{22} & A_{23} & 0 & 0 & 0 \\ A_{31} & A_{32} & A_{33} & 0 & 0 & 0 \\ 0 & 0 & 0 & G_{yz} & 0 & 0 \\ 0 & 0 & 0 & 0 & G_{zx} & 0 \\ 0 & 0 & 0 & 0 & 0 & G_{xy} \end{pmatrix}, \tag{6.1}$$

with the shear moduli G_{xy}, G_{yz}, G_{zx} and the entries A_{ij} depending on the elastic moduli E_x, E_y, E_z and the Poisson's ratios $\nu_{xy}, \nu_{yz}, \nu_{zx}$. The exact formula for A_{ij} can be found in [30, Chap. 2.4].

Some important differences compared to isotropic material laws are worth pointing out. While in the isotropic case, all Poisson's ratios share the same value, for orthotropic materials they represent three independent material parameters. The only relation between the ratios is $\nu_{ij}E_j = \nu_{ji}E_i$. Also the possible range of the material parameters, i.e., $-1 < \nu < 1/2$ for the isotropic case, is different. A positive definite stiffness tensor and thus a coercive energy functional is only guaranteed if $1 > \nu_{yz}^2 E_z/E_y + \nu_{xy}^2 E_y/E_x + 2\nu_{xy}\nu_{yz}\nu_{zx}E_z/E_x + \nu_{zx}^2 E_z/E_x$ and $E_x/E_y > \nu_{xy}^2$. Note that Poisson's ratios larger than $1/2$ are permitted, but this does not imply unphysical behavior as in the isotropic case, see, e.g., [31]. The conditions $E_i, G_{ij} > 0$ hold both in the isotropic and orthotropic case.

The curved domain of the violin bridge can be very precisely described by a spline volume. Since it is not suitable for a single-patch description, we decompose it into 16 three-dimensional spline patches shown in Fig. 6.3. While the description of the geometry could also be done with fewer patches, the number of 16 patches Ω_l gives us regular geometry mappings and a reasonable flexibility of the individual meshes.

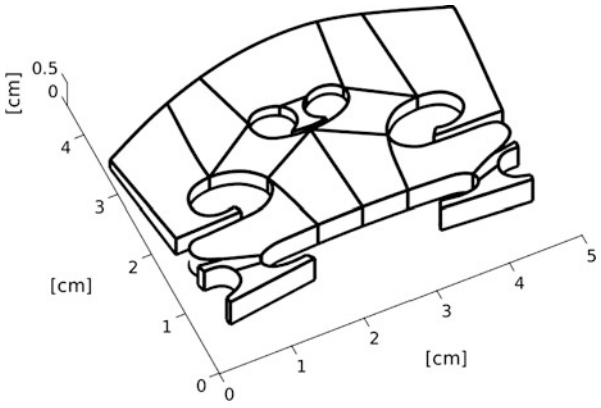

Fig. 6.3 Decomposition of the three-dimensional geometry into 16 patches Ω_l and 16 interfaces γ_k

The decomposed geometry is solved using an equal-order isogeometric mortar method as described in [4]. A trivariate B-spline space V_l is considered on each patch Ω_l. The broken ansatz space $V_h = \prod_l V_l$ is weakly coupled on each of the 16 interfaces. For each interface γ_k the two adjacent domains are labeled as one slave and one master domain (i.e. $\gamma_k = \partial\Omega_{s(k)} \cap \partial\Omega_{m(k)}$) and the coupling space M_k is set as a reduced trace space of the spline spaces on the slave domain, i.e., $M_h = \prod_k M_k$. Several crosspoints and wirebasket lines exist in the decomposition where an appropriate local degree reduction has to be performed to guarantee uniform stability, see [4, Sect. 4.3].

We use the standard bilinear forms for mortar techniques in linear elasticity

$$a(u,v) = \sum_l \int_{\Omega_l} \sigma(u) : \varepsilon(v), \quad m(u,v) = \sum_l \int_{\Omega_l} \rho u v, \quad b(v,\widehat{\tau}) = \sum_k \int_{\gamma_k} [v]_k \widehat{\tau},$$

where $[v]_k = v_{s(k)}\big|_{\gamma_k} - v_{m(k)}\big|_{\gamma_k}$ denotes the jump across the interface γ_k. We note that no additional variational crime by different non-matching geometrical resolutions of γ_k enters. The detailed eigenvalue problem is defined as $(u,\tau) \in V_h \times M_h$, $\lambda \in \mathbb{R}$, such that

$$a(u,v) + b(v,\tau) = \lambda m(u,v), \qquad v \in V_h, \tag{6.2a}$$

$$b(u,\widehat{\tau}) = 0, \qquad \widehat{\tau} \in M_h. \tag{6.2b}$$

We note that the constraint (6.2b) reflects the weak continuity condition of the displacement across the interface with respect to the standard two-dimensional Lebesgue measure. Only in very special situations strong point-wise continuity is granted from (6.2b).

6.2.2 Transforming Geometrical Parameters to Material Parameters

Additional to the nine material parameters E_i, G_{ij}, ν_{ij}, we consider a geometry parameter μ_{10} related to the thickness of the violin bridge. Transforming the geometry to a reference domain, we can interpret the thickness parameter as extra material parameter. Let the parameter dependent geometry $\Omega(\mu)$ be a uni-directional scaling of a reference domain $\widehat{\Omega}$, i.e., a transformation by $F(\cdot;\mu) : \widehat{\Omega} \to \Omega(\mu)$, $\mathbf{x} = F(\widehat{\mathbf{x}};\mu) = (\widehat{x},\widehat{y},\mu_{10}\widehat{z})$, with $\widehat{\mathbf{x}} = (\widehat{x},\widehat{y},\widehat{z}) \in \widehat{\Omega}$. Transforming the unknown displacement and rescaling it as $\widehat{u}(\widehat{\mathbf{x}}) = DF(\widehat{\mathbf{x}};\mu)^\top u(F(\widehat{\mathbf{x}};\mu))$ allows us to define a symmetric strain variable on the reference domain

$$\widehat{\varepsilon}(\widehat{u}(\widehat{\mathbf{x}})) = DF(\widehat{\mathbf{x}};\mu)^\top \varepsilon(u(F(\widehat{\mathbf{x}};\mu)))DF(\widehat{\mathbf{x}};\mu).$$

The orthotropic stiffness tensor (6.1) is then transformed to

$$\widehat{\mathbb{C}}(\mu) = \begin{pmatrix} A_{11} & A_{12} & \mu_{10}^{-2}A_{13} & & & \\ A_{21} & A_{22} & \mu_{10}^{-2}A_{23} & & & \\ \mu_{10}^{-2}A_{31} & \mu_{10}^{-2}A_{32} & \mu_{10}^{-4}A_{33} & & & \\ & & & \mu_{10}^{-2}G_{yz} & & \\ & & & & \mu_{10}^{-2}G_{zx} & \\ & & & & & G_{xy} \end{pmatrix}.$$

In terms of this coordinate transformation, the eigenvalue problem in the continuous H^1-setting reads, since $\det DF(\widehat{\mathbf{x}};\mu) = \mu_{10}^{-1}$ is constant, as

$$\int_{\widehat{\Omega}} \widehat{\varepsilon}(\widehat{u})\, \widehat{\mathbb{C}}(\mu)\, \widehat{\varepsilon}(\widehat{v})\, \mathrm{d}\widehat{\mathbf{x}} = \lambda \int_{\widehat{\Omega}} \rho\, \widehat{u}^\top \begin{pmatrix} 1 & & \\ & 1 & \\ & & \mu_{10}^{-2} \end{pmatrix} \widehat{v}\, \mathrm{d}\widehat{\mathbf{x}}.$$

In the mortar case, the coupling conditions across the interfaces have to be transformed as well. Here we assume that the meshes on the physical domain are obtained from the same mesh on the reference domain by the mapping F.

$$\begin{aligned} \int_{\gamma(\mu)} [u(\mathbf{x})]\tau(\mathbf{x})\, \mathrm{d}\gamma(\mathbf{x}) &= \int_{\widehat{\gamma}} [DF(\widehat{\mathbf{x}};\mu)^{-\top}\widehat{u}(\widehat{\mathbf{x}})]\tau(F(\widehat{\mathbf{x}};\mu))\mu_{10}\, \mathrm{d}\widehat{\gamma}(\widehat{\mathbf{x}}) \\ &= \mu_{10} \int_{\widehat{\gamma}} [\widehat{u}(\widehat{\mathbf{x}})] \begin{pmatrix} 1 & & \\ & 1 & \\ & & \mu_{10}^{-1} \end{pmatrix} \tau(F(\widehat{\mathbf{x}};\mu))\, \mathrm{d}\widehat{\gamma}(\widehat{\mathbf{x}}). \end{aligned}$$

We note that $\widehat{\tau} := \tau \circ F$ is in the parameter independent Lagrange multiplier space on the reference domain if τ is in the parameter dependent one on the physical domain. The remaining parameter dependence is a pure scaling of the Lagrange multiplier, which does not influence the constrained primal space. These considerations show us that the standard mortar coupling which is due to the geometry variation parameter dependent can be transformed to a parameter independent one.

While these lines use the special structure of the geometry variation F, the coupling can be transformed to a parameter independent one even in more general situations. Then, the coupling on $\Omega(\mu)$ must be posed in a suitable weighted L^2-space, which is adapted such that the transformed coupling is parameter independent.

Another material parameter is the constant mass density ρ. However it does not influence the eigenvectors. Only the eigenvalue is rescaled, yielding a trivial parameter dependence. For this reason, the density is kept constant in the reduced basis computations and can be varied in a post-process by rescaling the eigenvalues.

The described material parameters allow for an affine parameter dependence of the mass and the stiffness, with $Q_a = 10$, $Q_m = 2$,

$$a(\cdot,\cdot;\mu) = \sum_{q=1}^{Q_a} \theta_a^q(\mu) a^q(\cdot,\cdot), \quad m(\cdot,\cdot;\mu) = \sum_{q=1}^{Q_m} \theta_m^q(\mu) m^q(\cdot,\cdot),$$

where $\theta_m^1(\mu) = 1$ can be chosen parameter independent.

6.3 Reduced Basis

We now apply reduced basis (RB) methods for the approximation of the parameter dependent eigenvalue problem on the reference domain. By abuse of notation, we denote the spaces and bilinear forms transformed to the reference domain as before. RB techniques where the detailed problem is in saddle point form, in general, require the construction of RB for both the primal and the dual space, see, e.g., variational inequalities or when the coupling is parameter dependent, see [12, 14, 15, 25]. To ensure the inf-sup stability of the discrete saddle point problem, supremizers can be added to the primal space, additionally increasing the size of the reduced system, see [32, 34]. Here it is sufficient to define a RB for the primal space. For the simultaneous approximation of possible multiple eigenvalues and eigenvectors, we follow the approach given and analyzed in [17].

Due to the parameter independence of $b(\cdot,\cdot)$ and the dual space, obtained by the transformation described above, we can reformulate the detailed saddle point problem (6.2) in a purely primal form posed on the constrained space

$$X_h = \{v \in V_h, b(v,\widehat{\tau}) = 0, \widehat{\tau} \in M_h\}.$$

We recall that this formulation is not suitable for solving the detailed solution, since, in general, it is costly to construct explicitly a basis of X_h and severely disturbs the sparsity of the detailed matrices.

The construction of the RB functions is done in two steps. Firstly, an initial basis is built by a small POD from detailed solutions. This basis is then enlarged by a greedy algorithm using an asymptotically reliable error estimator. All detailed solutions do satisfy the weak coupling property and by definition the RB functions do as well. Thus the saddle-point problem is reduced to a positive definite one. The eigenvalue problem on the reduced space $X_N = \{\zeta_n \in X_h, n = 1, \dots, N\}$, for the first K eigenpairs is then given by: Find the eigenvalues $\lambda_{\mathrm{red},i}(\mu) \in \mathbb{R}$ and the eigenfunctions $u_{\mathrm{red},i}(\mu) \in X_N$, $i = 1, \dots, K$, such that

$$a(u_{\mathrm{red},i}(\mu), v; \mu) = \lambda_{\mathrm{red},i}(\mu)\, m(u_{\mathrm{red},i}(\mu), v; \mu), \quad v \in X_N.$$

The error estimator presented in [17, Corollary 3.3] can directly be applied, but the online-offline decomposition needs to be modified. In the original setting, a parameter independent mass was considered, so we need to additionally include the affine decomposition of the mass matrix.

The definition of the estimator is based on the residual

$$r_i(\cdot; \mu) = a(u_{\mathrm{red},i}(\mu), \cdot; \mu) - \lambda_{\mathrm{red},i}(\mu)\, m(u_{\mathrm{red},i}(\mu), \cdot; \mu)$$

measured in the dual norm $\|\cdot\|_{\hat{\mu};X_h'}$, with $\|g\|_{\hat{\mu};X_h'} = \sup_{v \in X_h} g(v)/\hat{a}(v,v)^{1/2}$ for $g \in X_h'$, where $\hat{a}(u,v) := a(u, v; \widehat{\mu})$, and $\widehat{\mu} \in \mathscr{P}$ is a reference parameter. We define $\hat{e}_i(\mu) \in X_h$ by

$$\hat{a}(\hat{e}_i(\mu), v) = r_i(v; \mu), \quad v \in X_h.$$

To adapt the online-offline decomposition, we follow [17, 23] and add additional terms corresponding to the mass components $m^q(\cdot,\cdot)$. The decomposition of the mass can be related to the already known decomposition of the stiffness matrix, by formally defining a bilinear form $a(u, v; \mu) - \lambda_{\mathrm{red},i}(\mu)\, m(u, v; \mu)$. For the convenience of the reader we recall the main steps. Let $(\zeta_n)_{1 \le n \le N}$ be a orthonormal basis (w. r. t. $m(\cdot,\cdot;\widehat{\mu})$) of X_N and let us define $\xi_n^q \in X_N$ and $\xi_n^{m,q} \in X_N$ by

$$\hat{a}(\xi_n^q, v) = a^q(\zeta_n, v), \quad v \in X_h,\ 1 \le n \le N,\ 1 \le q \le Q_a,$$
$$\hat{a}(\xi_n^{m,q}, v) = m^q(\zeta_n, v), \quad v \in X_h,\ 1 \le n \le N,\ 1 \le q \le Q_m.$$

In the following, we identify the function $u_{\mathrm{red},i}(\mu) \in V_N$ and its vector representation w. r. t. the basis $(\zeta_n)_{1 \le n \le N}$ such that $(u_{\mathrm{red},i}(\mu))_n$ denotes the nth coefficient.

Then, given a reduced eigenpair $(u_{\mathrm{red},i}(\mu), \lambda_{\mathrm{red},i}(\mu))$, we have the error representation

$$\hat{e}_i(\mu) = \sum_{n=1}^{N} \sum_{q=1}^{Q_a} \theta_a^q(\mu) \left(u_{\mathrm{red},i}(\mu)\right)_n \xi_n^q - \lambda_{\mathrm{red},i}(\mu) \sum_{n=1}^{N} \sum_{q=1}^{Q_m} \theta_m^q(\mu) \left(u_{\mathrm{red},i}(\mu)\right)_n \xi_n^{m,q}.$$

Consequently, using $\|r_i(\cdot;\mu)\|^2_{\hat{\mu};X_h'} = \hat{a}(\hat{e}_i(\mu), \hat{e}_i(\mu))$, the computational cost intense part of the error estimator can be performed in the offline phase, see [17, Sect. 3.3] for a more detailed discussion.

6.4 Numerical Simulation

In this section, the performance of the proposed algorithm is illustrated by numerical examples. The detailed computations were performed using geoPDEs [6], a Matlab toolbox for isogeometric analysis, the reduced computations are based on RBmatlab [9].

For the detailed problem, we use an anisotropic discretization. In plane, we use splines of degree $p = 3$ on the non-matching mesh shown in Fig. 6.4. The mesh has been adapted locally to better resolve possible corner singularities of the solution. In the z-direction a single element of degree $p = 4$ is used. The resulting equation system has 45,960 degrees of freedom for the displacement whereas the surface traction on the interfaces is approximated by 2025 degrees of freedom.

We consider the ten parameters, described in Sect. 6.2, $\mu = (\mu_1, \ldots, \mu_{10})$ with the elastic modulii $\mu_1 = E_x$, $\mu_2 = E_y$, $\mu_3 = E_z$, the shear modulii $\mu_4 = G_{yz}$, $\mu_5 = G_{xz}$, $\mu_6 = G_{xy}$, Poisson's ratios $\mu_7 = \nu_{yz}$, $\mu_8 = \nu_{xz}$, $\mu_9 = \nu_{xy}$ and the scaling of the thickness μ_{10}.

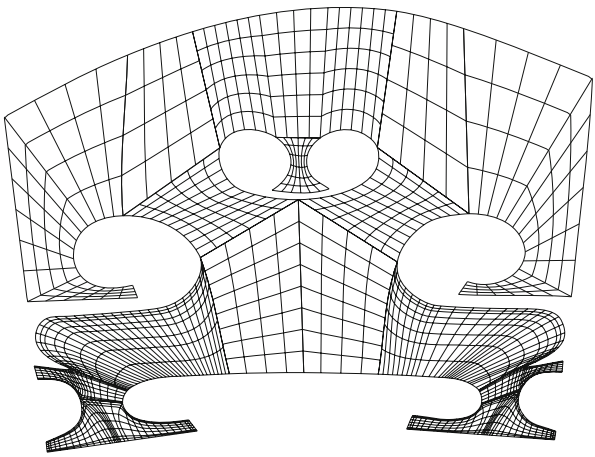

Fig. 6.4 Non-matching isogeometric mesh of the violin bridge

The considered parameter values were chosen according to real parameter data given in [31, Table 7-1]. We consider two different scenarios. In the first setting, we fix the wood type and take into account only natural variations, see [31, Sect. 7.10]. To capture the sensitivity of the violin bridge with respect to uncertainty in the material parameter one can chose a rather small parameter range around the reference parameter. We chose the reference data of *Fagus sylvatica*, the common beech, as given in Table 6.1, as well as the parameter range $\mathscr{P}_1$. The mass density is fixed in all cases as $720\,\mathrm{kg/m^3}$.

In our second test setting, we also consider different wood types. Hence we have to consider a larger parameter set, including the parameters for several types of wood, resulting in a larger parameter set $\mathscr{P}_2$, see Table 6.1. We note, that not all parameters in this large range are admissible for the orthotropic elasticity as they do not fulfill the conditions for the positive definiteness of the elastic tensor, stated in Sect. 6.2.1. Thus, we constrain the tensorial parameter space by

$$1 - \nu_{yz}^2 E_z/E_y + \nu_{xy}^2 E_y/E_x + 2\nu_{xy}\nu_{yz}\nu_{zx}E_z/E_x + \nu_{zx}^2 E_z/E_x \geq c_0,$$

as well as $E_x/E_y - \nu_{xy}^2 \geq c_1$ where the tolerances $c_0 = 0.01$ and $c_1 = 0.01$ were chosen, such that the wood types given in [31, Sect. 7.10] satisfy these conditions. Exemplary, in Fig. 6.5 we depict an lower-dimensional sub-manifold of $\mathscr{P}_2$ which includes non-admissible parameter values.

Table 6.1 Reference parameter and considered parameter ranges

	E_x [MPa]	E_y [MPa]	E_z [MPa]	G_{yz} [MPa]	G_{zx} [MPa]	G_{xy} [MPa]	ν_{yz}	ν_{zx}	ν_{xy}
$\widehat{\mu}$	14,000	2280	1160	465	1080	1640	0.36	0.0429	0.448
$\mathscr{P}_1$	13,000	1500	750	100	500	1000	0.3	0.03	0.4
	−15,000	−3000	−1500	−1000	−1500	−2000	−0.4	−0.06	−0.5
$\mathscr{P}_2$	1000	100	100	10	100	100	0.1	0.01	0.3
	−20,000	−5000	−2000	−5000	−2500	−5000	−0.5	−0.1	−0.5

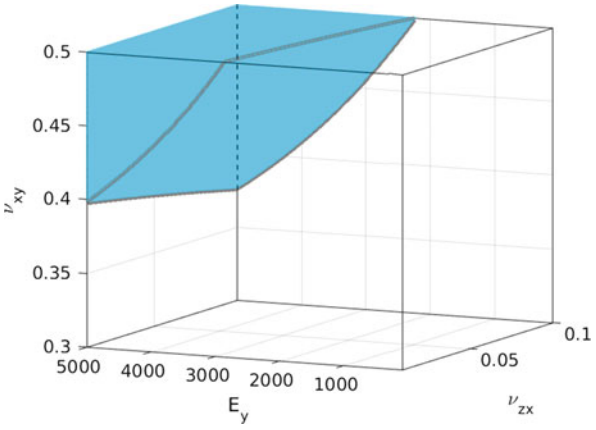

Fig. 6.5 Illustration of non-admissible parameter values in a lower-dimensional sub-manifold of $\mathscr{P}_2$, varying $\nu_{zx} \in (0.01, 0.1)$, $\nu_{xy} \in (0.3, 0.5)$, $E_y \in (100, 5000)$ and fixing $E_x = 1000$, $E_z = 2000$ and $\nu_{yz} = 0.5$

Table 6.2 The ten smallest eigenvalues for different thickness parameters, with the other parameters fixed to the reference value

Eigenvalue	$\mu_{10} = 0.5$	$\mu_{10} = 1.0$	$\mu_{10} = 2.0$	Ratio 0.5/1.0	Ratio 1.0/2.0
1	0.4057	1.3238	3.6954	0.3065	0.3582
2	1.1613	3.8870	10.8071	0.2988	0.3597
3	4.4096	12.9562	26.5621	0.3403	0.4878
4	6.1371	19.3254	30.0050	0.3176	0.6441
5	13.5564	27.3642	53.2657	0.4954	0.5137
6	19.2229	46.2521	93.9939	0.4156	0.4921
7	27.6118	65.0940	111.6075	0.4242	0.5832
8	39.3674	96.8069	129.3406	0.4067	0.7485
9	57.8266	107.6749	189.6090	0.5370	0.5679
10	68.0131	130.8876	241.7695	0.5196	0.5414

The thickness parameters is chosen to vary between 1/2 and 2 with the reference value set to 1

First, we consider the effect of the varying thickness parameter on the solution of our model problem. In Table 6.2 the first eigenvalues are listed for different values of the thickness, where we observe a notable and nonlinear parameter dependency. A selection of the corresponding eigenfunctions is depicted in Fig. 6.6, where the strong influence becomes even more evident, since in some cases the shape of the eigenmode changes when varying the thickness.

In the following RB tests, the relative error values are computed as the mean value over a large amount of random parameters. The L^2-error of the normed eigenfunctions is evaluated as the residual of the L^2-projection onto the corresponding detailed eigenspace. This takes into account possible multiple eigenvalues and the invariance with respect to a scaling by (-1).

The first test is the simultaneous approximation of the first five eigenpairs on both parameter sets $\mathscr{P}_1$ and $\mathscr{P}_2$. We use an initial basis of size 25 computed by a POD, which is enriched by the greedy algorithm up to a basis size of 250. In Fig. 6.7, the error decay for the different eigenvalues and eigenfunctions is presented. We observe very good convergence, with a similar rate in all cases. As expected the magnitude of the error grows with the dimension and range of the parameter set.

At this point, for the sake of completeness, we also consider the effectivities of the error estimator and the resulting speed-up. For example using the parameter range $\mathscr{P}_1$ varying the thickness, effectivities are around 4–16. Using the largest RB of dimension 250, the computational speedup of the eigenvalue solver in Matlab is a factor of 552.

Also an approximation of a larger number of eigenpairs does not pose any unexpected difficulties. Error values for the eigenvalue and eigenfunction are shown

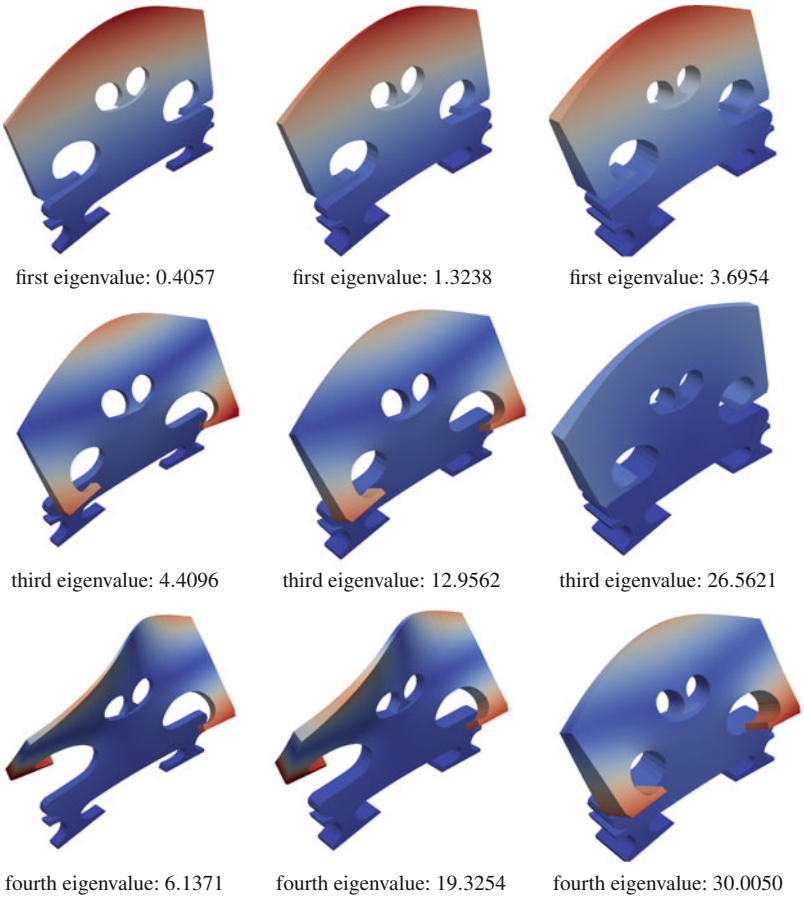

Fig. 6.6 Influence of the thickness of the bridge on several eigenfunctions

in Fig. 6.8 for an approximation of the first 15 eigenpairs in the parameter set $\mathscr{P}_1$, showing a good convergence behavior. The RB size necessary for a given accuracy increases compared to the previous cases of 5 eigenpairs, due to the higher amount of eigenfunctions which are, for a fixed parameter, orthogonal to each other.

When considering the relative error for the eigenvalues, see Figs. 6.7 and 6.8, we note that for a fixed basis size, the higher eigenvalues have a better relative approximation than the lower ones. In contrast, considering the eigenfunctions, the error of the ones associated with the lower eigenvalues are smaller compared to the

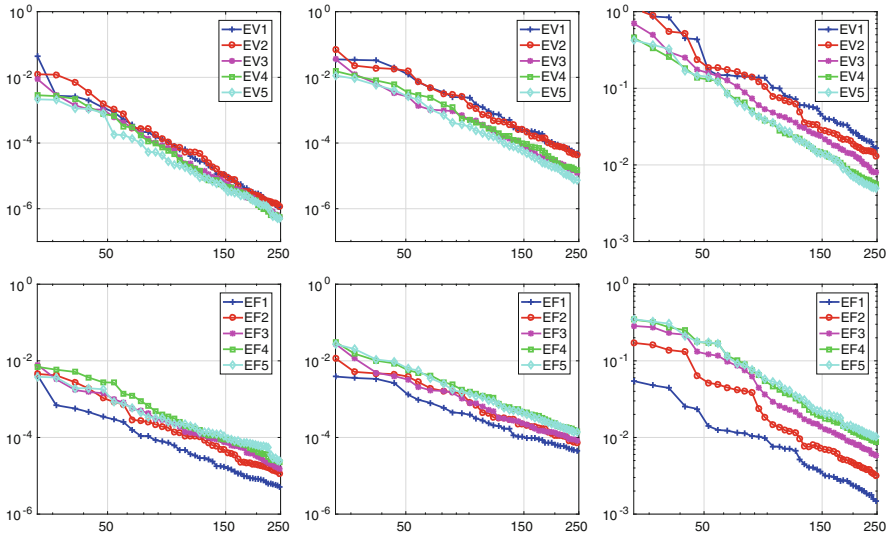

Fig. 6.7 Convergence of the relative error of the eigenvalues (*top*) and eigenfunctions (*bottom*). Parameter range $\mathscr{P}_1$ with a fixed thickness (*left*), with varying thickness (*middle*) and parameter range $\mathscr{P}_2$ with varying thickness (*right*)

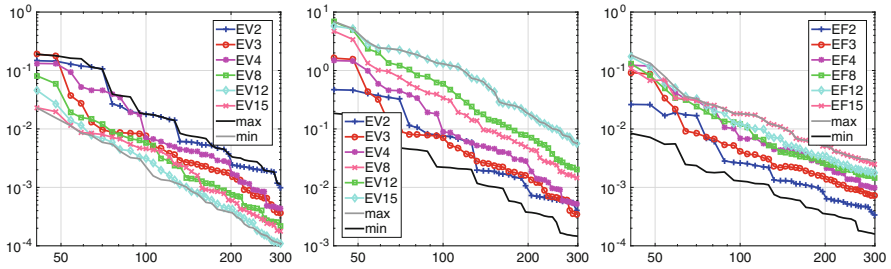

Fig. 6.8 Convergence of the relative (*left*), absolute (*middle*) error of the eigenvalues and eigenfunctions (*right*). Parameter range $\mathscr{P}_1$ with varying thickness, simultaneous approximating 15 eigenpairs

ones associated with the higher eigenvalues. This observation also holds true for the absolute error in the eigenvalues. This is related to the fact that eigenvalues depend sensitively on the parameters. In Fig. 6.9, we illustrate the distribution of the first and 15th eigenvalue.

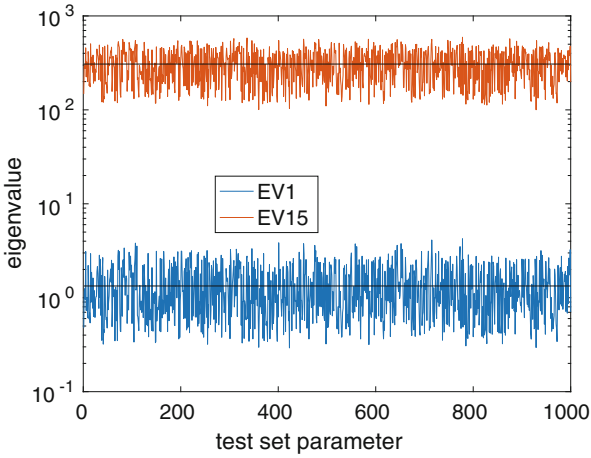

Fig. 6.9 Sampling of the first and 15th eigenvalue within the parameter set $\mathscr{P}_1$ as used in the test set. Extremal values: $\min \lambda_1 = 0.29$, $\max \lambda_1 = 4.24$, $\min \lambda_{15} = 100.19$, $\max \lambda_{15} = 593.65$

6.5 Conclusion

We have considered generalized eigenvalue problems to approximate the vibrations of parameter dependent violin bridges. The model reduction is carried out in terms of a RB method where the detailed solutions are obtained by isogeometric mortar finite elements. In all considered test scenarios, highly accurate approximations for both eigenvalues and eigenmodes are obtained. At the same time the complexity and thus the run-time is significantly reduced. Instead of a detailed saddle point system with 47,985 degrees of freedom, we have only to solve eigenvalue problems on positive-definite systems with less than 300 degrees of freedom. Of special interest is not only the variation in the material parameter but also to take into account possible changes in the thickness of the violin bridge. In terms of a mapping to a reference domain, we can reinterpret the geometry parameter as an additional material parameter and avoid the indefinite saddlepoint problem.

Acknowledgements We would like to gratefully acknowledge the funds provided by the "Deutsche Forschungsgemeinschaft" under the contract/grant numbers: WO 671/11-1, WO 671/13-2 and WO 671/15-1 (within the Priority Programme SPP 1748, "Reliable Simulation Techniques in Solid Mechanics. Development of Non-standard Discretisation Methods, Mechanical and Mathematical Analysis").

References

1. Beirão Da Veiga, L., Buffa, A., Sangalli, G., Vázquez, R.: Mathematical analysis of variational isogeometric methods. Acta Numer. **23**, 157–287 (2014)
2. Ben Belgacem, F., Maday, Y.: The mortar finite element method for three dimensional finite elements. Math. Model. Numer. Anal. **31**(2), 289–302 (1997)

3. Bernardi, C., Maday, Y., Patera, A.T.: A new nonconforming approach to domain decomposition: the mortar element method. In: Brezis, H. et al. (eds.) Nonlinear Partial Differential Equations and Their Applications, vol. XI, pp. 13–51. Collège de France, Paris (1994)
4. Brivadis, E., Buffa, A., Wohlmuth, B., Wunderlich, L.: Isogeometric mortar methods. Comput. Methods Appl. Mech. Eng. **284**, 292–319 (2015)
5. Cottrell, J.A., Hughes, T.J.R., Bazilevs, Y.: Isogeometric analysis. Towards Integration of CAD and FEA. Wiley, Chichester (2009)
6. de Falco, C., Reali, A., Vázquez, R.: GeoPDEs: a research tool for isogeometric analysis of PDEs. Adv. Eng. Softw. **42**(12), 1020–1034 (2011)
7. Dittmann, M., Franke, M., Temizer, I., Hesch, C.: Isogeometric analysis and thermomechanical mortar contact problems. Comput. Methods Appl. Mech. Eng. **274**, 192–212 (2014)
8. Dornisch, W., Vitucci, G., Klinkel, S.: The weak substitution method – an application of the mortar method for patch coupling in NURBS-based isogeometric analysis. Int. J. Numer. Methods Eng. **103**(3), 205–234 (2015)
9. Drohmann, M., Haasdonk, B., Kaulmann, S., Ohlberger, M.: A software framework for reduced basis methods using DUNE -RB and RBmatlab. Advances in DUNE, pp. 77–88. Springer, Berlin (2012)
10. Fletcher, N.H., Rossing, T.: The Physics of Musical Instruments, 2nd edn. Springer, New York (1998)
11. Fumagalli, I., Manzoni, A., Parolini, N., Verani, M.: Reduced basis approximation and a posteriori error estimates for parametrized elliptic eigenvalue problems. ESAIM: Math. Model. Numer. Anal. **50**, 1857–1885 (2016)
12. Gerner, A.L., Veroy, K.: Certified reduced basis methods for parametrized saddle point problems. SIAM J. Sci. Comput. **34**(5), A2812–A2836 (2012)
13. Glas, S., Urban, K.: On non-coercive variational inequalities. SIAM J. Numer. Anal. **52**, 2250–2271 (2014)
14. Glas, S., Urban, K.: Numerical investigations of an error bound for reduced basis approximations of noncoercice variational inequalities. IFAC-PapersOnLine **48**(1), 721–726 (2015)
15. Haasdonk, B., Salomon, J., Wohlmuth, B.: A reduced basis method for parametrized variational inequalities. SIAM J. Numer. Anal. **50**, 2656–2676 (2012)
16. Hesch, C., Betsch, P.: Isogeometric analysis and domain decomposition methods. Comput. Methods Appl. Mech. Eng. **213–216**, 104–112 (2012)
17. Horger, T., Wohlmuth, B., Dickopf, T.: Simultaneous reduced basis approximation of parameterized elliptic eigenvalue problems. ESAIM: Math. Model. Numer. Anal. **51**, 443–465 (2017)
18. Hughes, T.J.R., Cottrell, J.A., Bazilevs, Y.: Isogeometric analysis: CAD, finite elements, NURBS, exact geometry and mesh refinement. Comput. Methods. Appl. Mech. Eng. **194**, 4135–4195 (2005)
19. Hughes, T.J.R., Evans, J.A., Reali, A.: Finite element and NURBS approximations of eigenvalue, boundary-value, and initial-value problems. Comput. Methods Appl. Mech. Eng. **272**, 290–320 (2014)
20. Iapichino, L., Quarteroni, A., Rozza, G., Volkwein, S.: Reduced basis method for the Stokes equations in decomposable domains using greedy optimization. In: European Conference Mathematics in Industry, ECMI 2014, pp. 1–7 (2014)
21. Jansson, E.V.: Violin frequency response – bridge mobility and bridge feet distance. Appl. Acoust. **65**(12), 1197–1205 (2004)
22. Lovgren, A., Maday, Y., Ronquist, E.: A reduced basis element method for the steady Stokes problem. Math. Model. Numer. Anal. **40**, 529–552 (2006)
23. Machiels, L., Maday, Y., Oliveira, I.B., Patera, A.T., Rovas, D.V.: Output bounds for reduced-basis approximations of symmetric positive definite eigenvalue problems. C.R. Acad. Sci., Paris, Sér. I **331**(2), 153–158 (2000)
24. Milani, R., Quarteroni, A., Rozza, G.: Reduced basis method for linear elasticity problems with many parameters. Comput. Methods Appl. Mech. Eng. **197**(51–52), 4812–4829 (2008)
25. Negri, F., Manzoni, A., Rozza, G.: Reduced basis approximation of parametrized optimal flow control problems for the Stokes equations. Comput. Math. Appl. **69**(4), 319–336 (2015)

26. Pau, G.: Reduced-basis method for band structure calculations. Phys. Rev. E **76**, 046704 (2007)
27. Pau, G.: Reduced basis method for simulation of nanodevices. Phys. Rev. B **78**, 155425 (2008)
28. Quarteroni, A.: Numerical Models for Differential Problems, MS&A, vol. 8, 2nd edn. Springer, Milan (2014)
29. Quarteroni, A., Manzoni, A., Negri, F.: Reduced Basis Methods for Partial Differential Equations. An Introduction. Springer, New York (2015)
30. Rand, O., Rovenski, V.: Analytical Methods in Anisotropic Elasticity: With Symbolic Computational Tools. Birkhäuser, Boston (2007)
31. Ranz, T.: Ein feuchte- und temperaturabhängiger anisotroper Werkstoff: Holz. Beiträge zur Materialtheorie. Universität der Bundeswehr München (2007)
32. Rozza, G., Veroy, K.: On the stability of the reduced basis method for Stokes equations in parametrized domains. Comput. Methods. Appl. Mech. Eng. **196**, 1244–1260 (2007)
33. Rozza, G., Huynh, D.B.P., Patera, A.T.: Reduced basis approximation and a posteriori error estimation for affinely parametrized elliptic coercive partial differential equations. Application to transport and continuum mechanics. Arch. Comput. Methods Eng. **15**(3), 229–275 (2008)
34. Rozza, G., Huynh, D.B.P., Manzoni, A.: Reduced basis approximation and a posteriori error estimation for Stokes flows in parametrized geometries: roles of the inf-sup stability constants. Numer. Math. **125**(1), 115–152 (2013)
35. Seitz, A., Farah, P., Kremheller, J., Wohlmuth, B., Wall, W., Popp, A.: Isogeometric dual mortar methods for computational contact mechanics. Comput. Methods Appl. Mech. Eng. **301**, 259–280 (2016)
36. Vallaghe, S., Huynh, D.P., Knezevic, D.J., Nguyen, T.L., Patera, A.T.: Component-based reduced basis for parametrized symmetric eigenproblems. Adv. Model. Simul. Eng. Sci. **2** (2015)
37. Woodhouse, J.: On the "bridge hill" of the violin. Acta Acust. United Acust. **91**(1), 155–165 (2005)